Safety Assessment and Multi-Objective Optimization of a Paratransit Bus Structure

Cezary Bojanowski[1a]
Ronald F. Kulak[1b, 2]

1) *Transportation Research and Analysis Computing Center,*
Energy System Division
Argonne National Laboratory
2700 International Drive, Suite 201
West Chicago, IL 60185, USA
a) cbojanowski@anl.gov *b) kulak@anl.gov*

2) *RFK Engineering Mechanics Consultants*
307 Warwick Drive
Naperville, IL 60565, USA
rfkemc@aol.com

Abstract

Paratransit buses are used in the U.S. as a complementary service for regularly scheduled routes and are usually designed to transport disabled passengers in their wheelchairs. Paratransit buses consist of custom passenger compartments mounted onto separate cutaway chassis--usually built by reputable manufacturer like Ford or GM--by a secondary manufacturer called a "body builder". The lack of dedicated national crashworthiness standards, along with different construction methods used by paratransit fleet manufacturers, can result in a wide variance of passenger compartment structural strength. To ensure adequate crashworthiness performance, in August 2007 the Florida Department of Transportation (FDOT) introduced a standard stipulating that newly acquired buses must be tested for rollover and side impact conditions. The rollover test is performed using a tilt table test according to UN-ECE Regulation 66. The side impact test involves the impact of a bus by a common SUV or pickup truck.

In the current study, a detailed FE model of a paratransit bus was used to perform LS-DYNA® explicit simulations of both rollover and side impact testing procedures per FDOT standard. LSTC IIHS solid movable barrier was adapted for the side impact test. Based on the results, the safety level of the bus was assessed. Subsequently, the response of the bus structure in the two impact scenarios together with the total mass were used as three separate objectives in a trade-off optimization study within LS-OPT®. The Pareto solutions were identified and presented using the newly implemented Hyper-Radial Visualization method in LS-OPT.

The simulation results show that the original bus design would pass the FDOT testing procedure. However, appropriate redistribution of the mass can noticeably increase its strength.

Keywords: *Rollover, Side impact, LSTC IIHS barrier, Paratransit bus, Multi-objective optimization, Crashworthiness optimization*

1. Introduction

Paratransit buses are used in the U.S. as a complementary service for regularly scheduled routes and are usually designed to transport disabled passengers in their wheelchairs. Unlike the monolithic construction of a larger bus, a paratransit buses are built in two distinct stages. They consist of custom passenger compartments mounted onto separate cutaway chassis, like the Ford E-450 chassis shown in Figure 1a. Passenger compartments are assembled on the chassis by a secondary manufacturer. An example of a steal frame of a passenger compartment is presented in Figure 1b. With the two stage assembly process and medium Gross Vehicle Weight around 10,000 lbs, paratransit buses are excluded from the scope of many crashworthiness related domestic and international standards. However, in 2007 the Florida Department of Transportation (FDOT) together with FAMU-FSU College of Engineering introduced a standard that requires newly acquired buses to be tested for rollover and side impact conditions [1]. To a large extent, the rollover testing procedure is derived from UN-ECE Regulation 66 (R66) [2]. The side impact test involves the impact of a bus by a common SUV or pickup truck. Penetration of the so called residual space is used as a failure criterion in both tests. In the FDOT standard, experimental testing and computational analysis are treated equivalently. The computational path requires documented verification and validation of the models used. Several tests at different levels of model complexity (i.e. unit, subsystem and full model levels) were proposed to help validate the models and also identify weak points in the design [3].

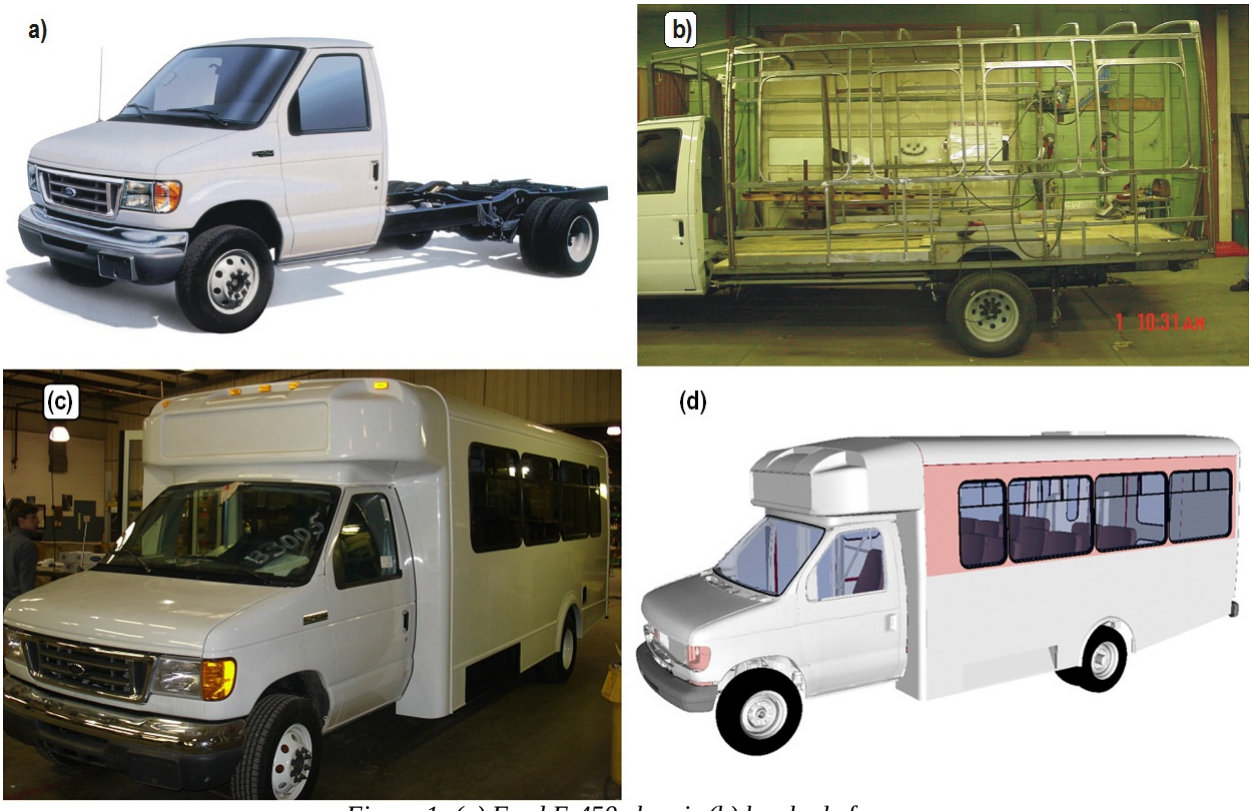

Figure 1: (a) Ford E-450 chassis (b) bus body frame
(c) Tested paratransit bus and its (d) finite element model representation

In the current study, a detailed FE element model (620,000 elements) of a common paratransit bus (Figure 1c and 1d) was used for the safety level estimation. Both, rollover and side impact

test simulations per FDOT standard were conducted using the LS-DYNA solver. These two impact scenarios were subsequently used in metamodel based multi-objective optimization in LS-OPT. The goal of this study was to identify the most relevant elements for the bus frame-strength and optimize their response in the rollover and the side impact tests.

2. Baseline Design Performance in Rollover Test Simulation

In the rollover test procedure, a vehicle resting on a tilting platform is quasi-statically rotated onto its weaker side. When the center of gravity reaches the highest (critical) point, the rotation of the table is ceased, and gravity causes the bus to free-fall into a ditch. The concrete flooring in the ditch is 800 mm beneath the tilt table's horizontal position. Figure 2a shows the unstable position of the bus and Figure 2b shows the position just before the contact with the ground. One full rollover simulation from the unstable position was performed to compute the velocities of the vehicle before impact. These velocities were subsequently used as initial conditions for simplified simulations (Figure 2b) in LS-OPT studies.

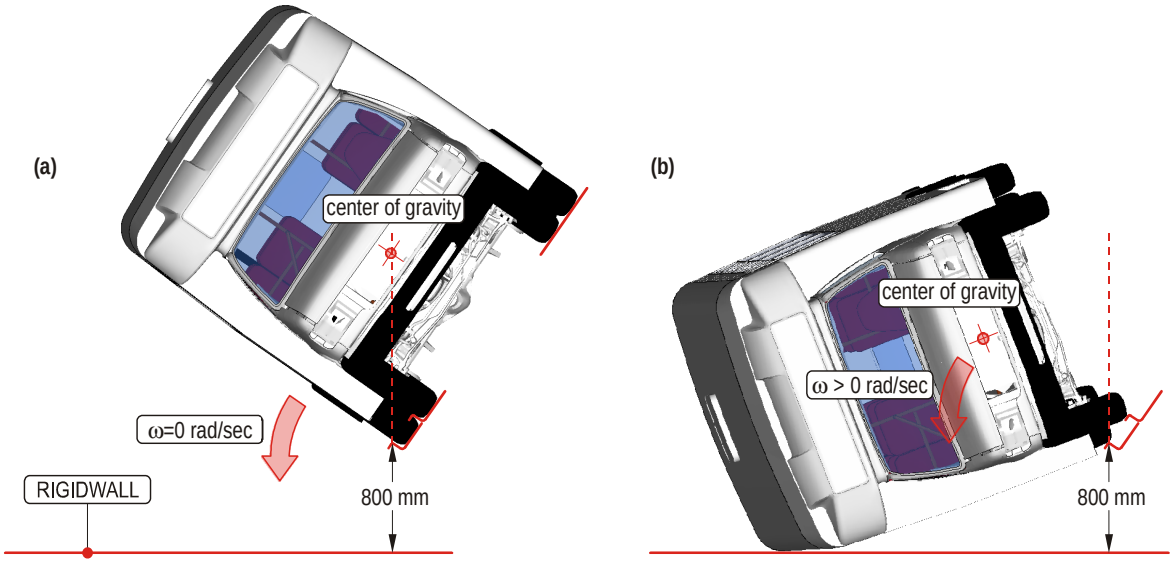

Figure 2: Initial conditions for the rollover simulations (a) full rollover (b) simplified simulation

A bus is considered to be crashworthy and safe if the residual space is not compromised during the tests [4-5]. The shape of the residual space is defined in Figure 3. For easier comparison of the results and the ability to quantitatively assess the deformation extent, the deformation index (DI), was proposed [3]. It is based on the assumption that during the rollover-induced impact, the angular deformations develop only in hypothetical plastic hinges. These hinges are marked on the bus cross section as α_1 throught α_6 in Figure 3. The elastic deformations of the walls are neglected in this definition. Based on the geometry of the failure mode (Figure 3b), DI is defined as:

$$DI = \frac{l}{d} \cdot \tan(\Delta\alpha_1) + \frac{(h-l)}{d} \cdot \tan(\Delta\alpha_2) \quad (1)$$

For acceptable designs, DI is in the range $0 \le DI < 1$. When $DI \ge 1$, the structure of the wall intrudes into the residual space, and the bus fails the test.

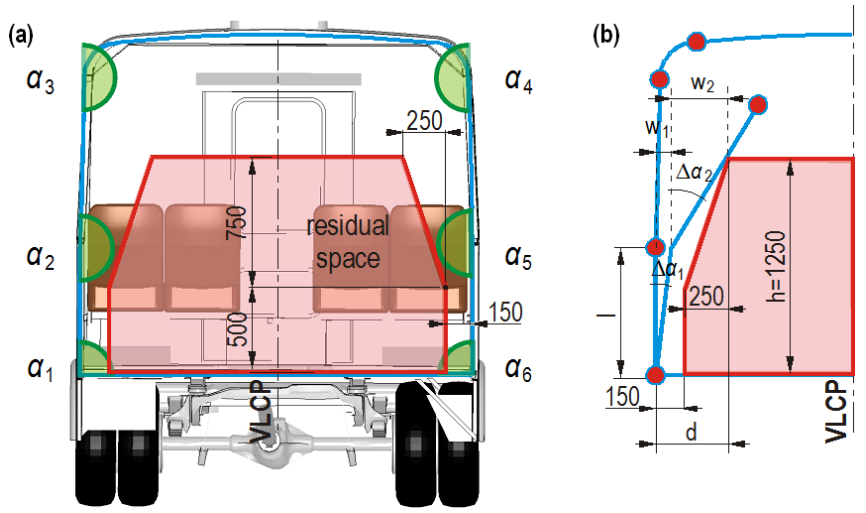

Figure 3: (a) Definition of the residual space (b) geometry of the failure mode [3]

The structure of the bus deformed in a torsion-like mode, with the frontal part twisting the most. Figure 4a shows the deformed cross section of the bus, and Figure 4b shows the histories of the angles α_1 and α_2 for the critical cross section. These plots were used to calculate $DI = 0.63$, which translates to 37% of remaining safety margin. The residual space was not penetrated in the test.

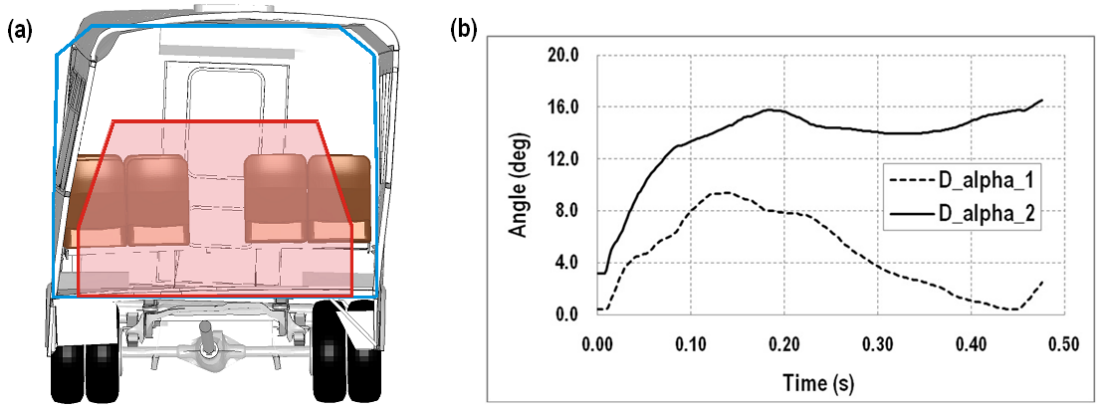

Figure 4: Deformation of the bus body in rollover simulation:
(a) cross section of maximum deformation (b) histories of the angles α_1 and α_2

3. Baseline Design Performance in Side Impact Test Simulation

For the side impact test, the FDOT standard proposes the use of common pickups or SUVs as impacting vehicles. However, the results may be inconsistent if different vehicles are selected in multiple tests. The barrier used by the IIHS in their approval tests has the shape designed to represent the front end geometry of a typical SUV or pickup truck used in US. Thus, for simplification of the FE model and repeatability of the results, the IIHS barrier was used in the current study. In the test, the IIHS barrier was moving with initial velocity of 30 mph (13.41 m/s) and an approach angle of 90 deg. The FE model is shown in Figure 5.

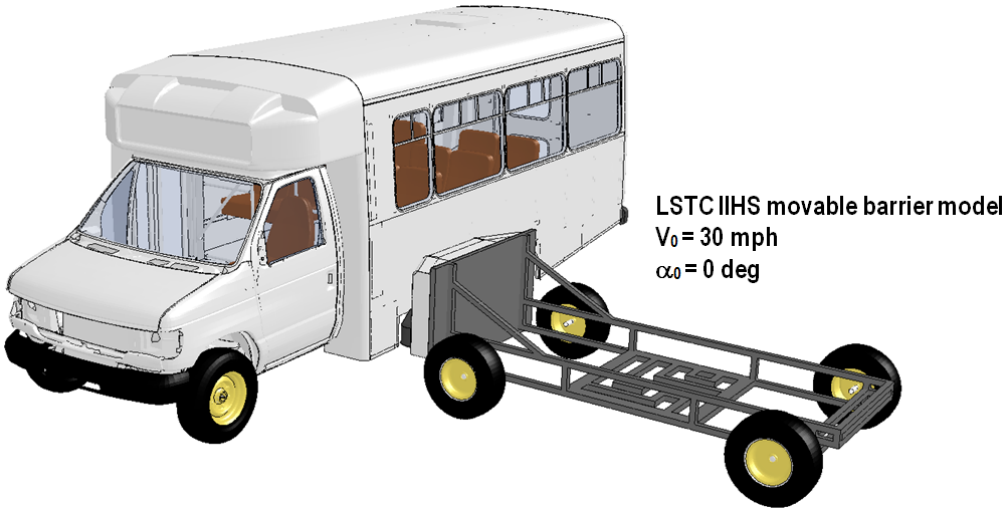

Figure 5: Model used for the side impact simulation

Figure 6 shows the location of the selected impact zone and the five check points for which intrusions were computed. If the maximum deformation measured at this level is greater than 150 mm, the residual space is infringed, and the bus fails the side impact test.

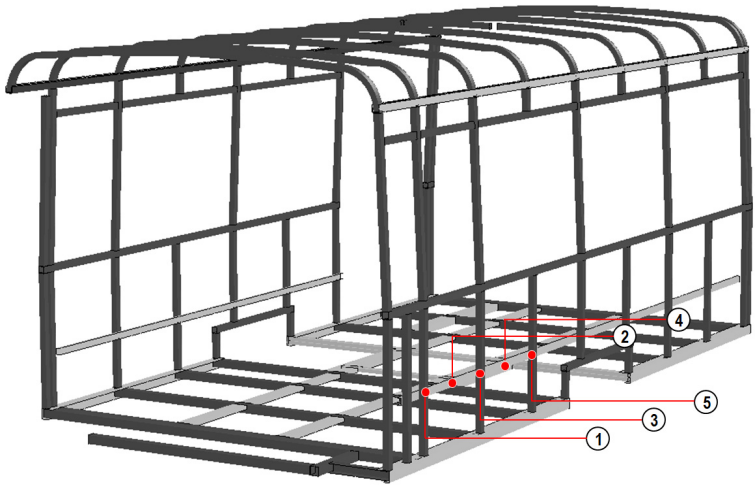

Figure 6: Location of the intrusion check points in the impact zone

Figure 7a shows the deformed cross section predicted by the side impact test simulation; Figure 7b presents measured intrusions. The maximum deformation was 79.1 mm, which translates to 47.3 % of safety margin. Thus, the bus tested would pass both rollover and side impact tests according to FDOT standard.

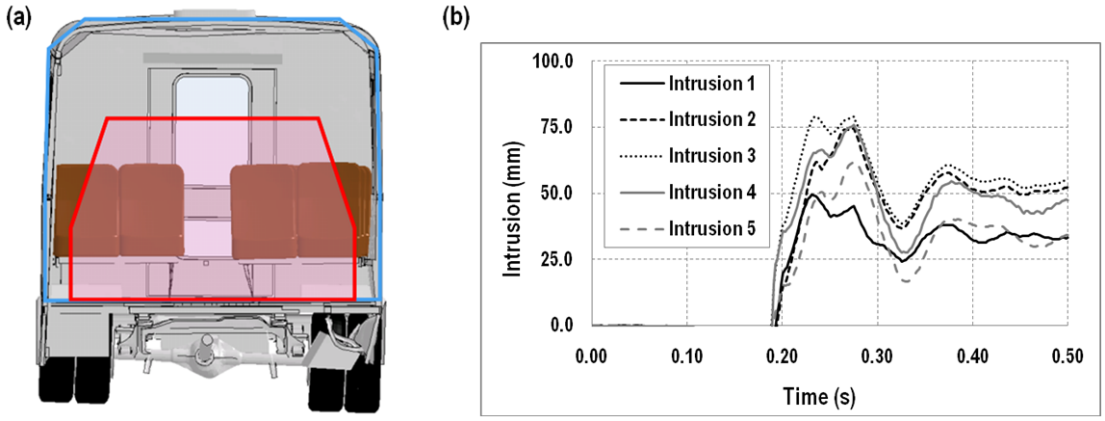

Figure 7: Deformation of the bus body in side impact simulation: (a) maximum deformation (b) intrusions in the wall structure

4. Multi-Objective Optimization

4.1. Problem Formulation

A general multi-objective discrete variables optimization can be mathematically formulated as:

$$\text{minimize:} \quad \boldsymbol{F}(\boldsymbol{x}) = [f_1(\boldsymbol{x}), f_2(\boldsymbol{x}), ..., f_t(\boldsymbol{x})] \tag{2}$$

$$\text{subject to:} \quad g_i(\boldsymbol{x}) = 0; \qquad i = 1, ..., p \tag{3}$$

$$g_j(\boldsymbol{x}) \le 0; \qquad j = 1, ..., q$$

$$x_k \in D_k, \qquad D_k = (d_{k1}, d_{k2}, ..., d_{kr}); \quad k = 1, ..., n$$

Where:

F – is the objective vector comprised of t objective functions,
g – are equality and inequality constraints in number of $p + q$,
D_k – is a feasible discrete set for kth discrete design variable x_k,

In the current study, three objective functions were identified and are given in Table 1. Minimization of the deformations in both rollover (1) and side impact (2) simulations naturally conflicted with the objective of minimization of the structure mass (3). The intrusion from side impact was scaled by 150 mm, so it takes the values between $0 \le intrusion\_max\_scaled < 1.0$ for acceptable results.

Table 1: Objectives of the optimization study

	Objective	***Symbol***	***Initial Design***
(1)	minimize mass of the frame	*mass*	0.388 tonne
(2)	minimize DI in rollover	*DI*	0.63
(3)	minimize scaled maximum intrusion in side impact	*intrusion_max_scaled*	0.53 (79.1 mm)

Figure 8 shows the passenger compartment frame with eight numbered parts. Thicknesses of elements in these parts were used in the optimization study as the design variables. The initial

values for them as well as assumed lower and upper bounds for optimization are shown in Table 2. The manufacturer used discrete "gauge" unit to specify sheet metal thickness. The conversion from gauge to inch and millimeter for structural elements made of galvanized steel is shown in Table 3.

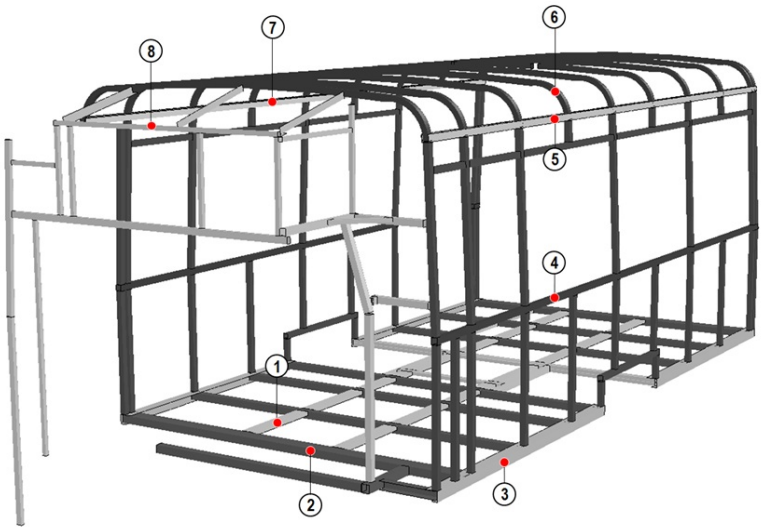

Figure 8: Location of the structural elements used in definition of design variables

Table 2: Variables used in the optimization process

	Variable	***Symbol***	***Baseline Design (ga)***	***Range of Values (ga)***
(1)	thickness of C-channel in the floor structure	*floor_c*	11	10 -17
(2)	thickness of square tubes in the floor structure	*floor_s*	13	10 -17
(3)	thickness of C-channel in the wall structure	*wall_c*	14	11-18
(4)	thickness of square tubes in the wall structure	*wall_s*	18	12-19
(5)	thickness of U-shapes in the roof structure	*roof_u*	18	12-19
(6)	thickness of S-shapes in the roof structure	*roof_s*	18	12-19
(7)	thickness of L-shapes in the roof structure	*roof_l*	11	10 -17
(8)	thickness of the elements in the front cap structure	*cap_s*	16	12-19

Table 3: Gauge to millimeter and inch conversion for galvanized steel

Gauge	***(in)***	***(mm)***	***Gauge***	***(in)***	***(mm)***
10	0.1382	3.510	**15**	0.071	1.803
11	0.1233	3.132	**16**	0.0635	1.613
12	0.1084	2.753	**17**	0.0575	1.461
13	0.0934	2.372	**18**	0.0516	1.311
14	0.0785	1.994	**19**	0.0456	1.158

To solve the problem, metamodel based optimization was used with sequential strategy. The responses were approximated using Radial Basis Function Network based on solutions obtained from sampling points distributed with space filling algorithm. Fourteen simulations per iteration per impact scenario were performed, and this resulted in total of 56 LS-DYNA calculations in two iterations.

4.2. Design Sensitivities

A sensitivity analysis provides information on the significance of a particular design variable on the response. This can be useful to identify the most relevant inputs and to reduce the number of variables in the optimization process. It may also help to better understand the performance of a system. Sensitivity analysis can be executed in LS-OPT 4.1 using Analysis Of Variance (ANOVA), Global Sensitivity Analysis (GSA) with Sobol's approach or coefficients of correlation [4]. In this study ANOVA and GSA were used. ANOVA plots are constructed in LS-OPT based on linear response surface fit. The true response $y(\boldsymbol{x})$ is approximated by the first order polynomial, $f(\boldsymbol{x})$, defined as:

$$f(\boldsymbol{x}) = \sum_{j=1}^{L} b_j \phi_j(\boldsymbol{x}) \tag{4}$$

Where:

$L-$ is the size of basis functions' vector ($\phi_j = [1, x_1, ..., x_n]^T$). The vector of constants $\boldsymbol{b}$ is determined through minimization of the sum of the square errors computed by:

$$\sum_{i=1}^{P} \left\{ [y_i(\boldsymbol{x}) - f_i(\boldsymbol{x})]^2 \right\} = \sum_{i=1}^{P} \left\{ \left[y_i(\boldsymbol{x}) - \sum_{j=1}^{L} b_j \phi_j(\boldsymbol{x}) \right]^2 \right\} \tag{5}$$

Where:

$f_i(\boldsymbol{x})-$ are responses predicted by metamodel,
$y_i(\boldsymbol{x})-$ are responses simulated by LS-DYNA,
$P-$ is the total number of sampling points.

ANOVA plots in LS-OPT represent normalized b_j coefficients with their confidence intervals. The $100(1-\alpha)\%$ confidence intervals for the coefficients b_j, $j = 0,1,...,L$ are defined through:

$$\beta_j \in \left[b_j - \frac{\Delta b_j(\alpha)}{2}, b_j + \frac{\Delta b_j(\alpha)}{2} \right] \tag{6}$$

Further definition of the confidence bounds can be found in [6].

For the cases, where interaction parameters play significant role in approximating the response, application of Sobol's Indices may be more suitable. This approach uses a unique decomposition of a function into summands with increasing dimensions as [5]:

$$f(x_1,...,x_n) = f_0 + \sum_{i=1}^{n} f_i(x_i) + \sum_{i=1}^{n} \sum_{j=i+1}^{n} f_{ij}(x_i, x_j) + ... + f_{1,2,...,n}(x_1,...,x_n) \tag{7}$$

Where:

$f(x_1,...,x_n)-$ is the analyzed model with *n* random variables.

Each random model response $f_k(x_1,...,x_n)$ is characterized by its variance D^k. This variance can be also decomposed into partial variances as:

$$D^k = \sum_{i=1}^{n} D_i^k + \sum_{i=1}^{n}\sum_{j=i+1}^{n} D_{ij}^k + ... + D_{1,2,...,n}^k \tag{8}$$

The Sobol's Indices are defined by:

$$S(i_1,..,i_s) = \frac{D_{i_1,...,i_s}^k}{D^k} \tag{9}$$

Where:

$S_i = \frac{D_i}{D} -$ is the main effect of the parameter and,

$S_{Ti} -$ is the total effect, which combines parameter's main effect and all the interactions involving that parameter.

Computation of components in Equation (7) involves multi-dimensional integration. In practice only the main and total effects are computed using the approximate formulas based on the Monte Carlo integrations [5].

Figures 9 to 11 show the sensitivity studies for all three objective functions using linear ANOVA and Sobol's approaches. For the rollover test, the most important design variables were the thicknesses of the front cap structure (*cap_s*) and the roof bows (*roof_s*). For the side impact performance, the most important design variables turned out to be the thicknesses of the side wall main tubes (*wall_s*), the C-channel connecting the wall to the floor (*wall_c*) and the square tubes in the floor structure (*floor_s*). For the *mass* the most important were the thicknesses of the main tubing from all the panels (roof, wall and floor).

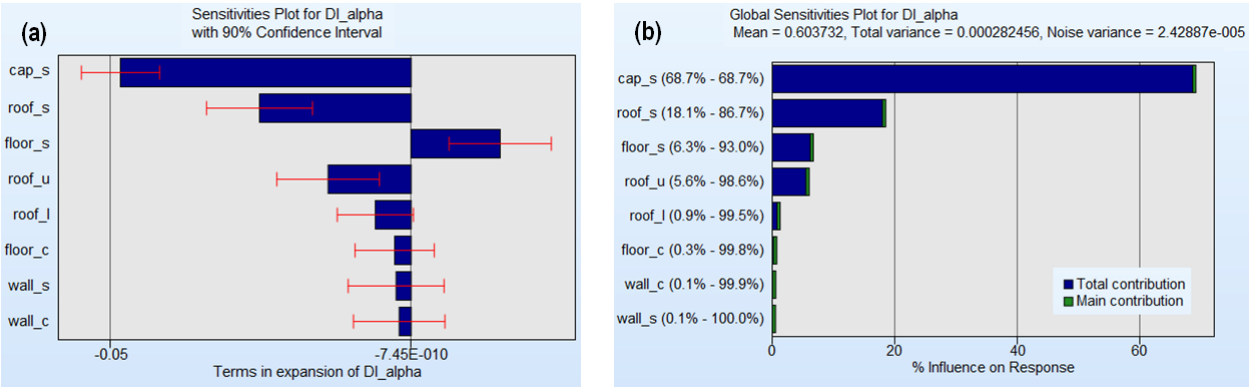

Figure 9: Sensitivity study for response DI based on (a) ANOVA (b) Sobol's Indices

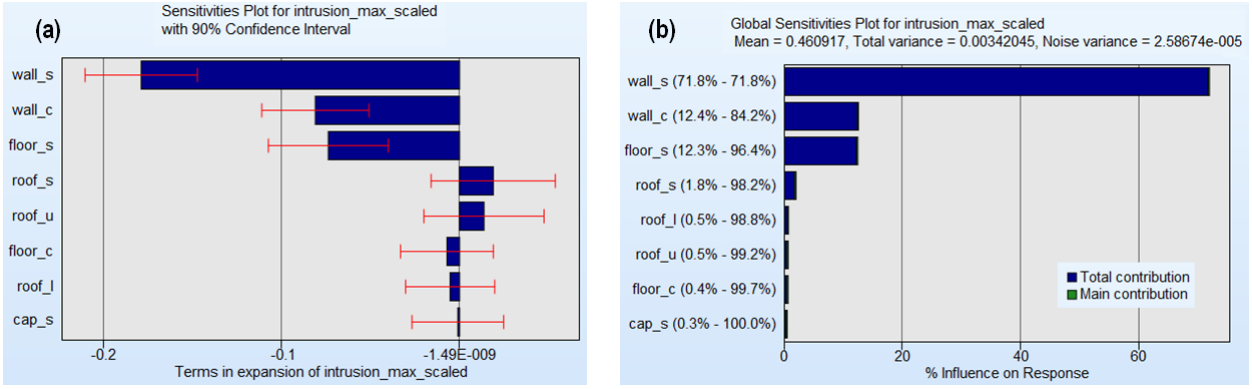

Figure 10: Sensitivity study for response intrusion_max_scaled based on (a) ANOVA (b) Sobol's Indices

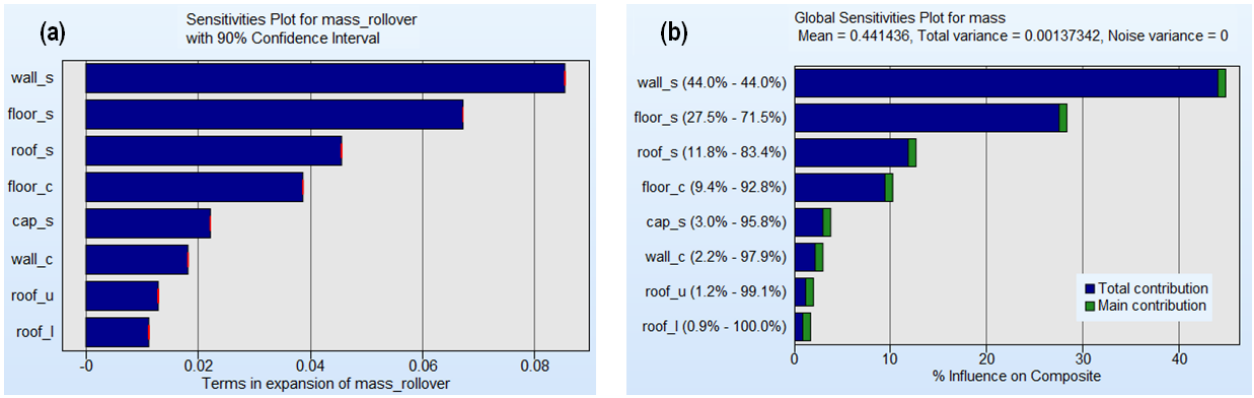

Figure 11: Sensitivity study for response mass based on (a) ANOVA (b) Sobol's Indices

Figure 12 shows cumulative sensitivity plots. Variations in only two input variables *wall_s* and *cap_s* account for ~63 % of the variations in all objectives.

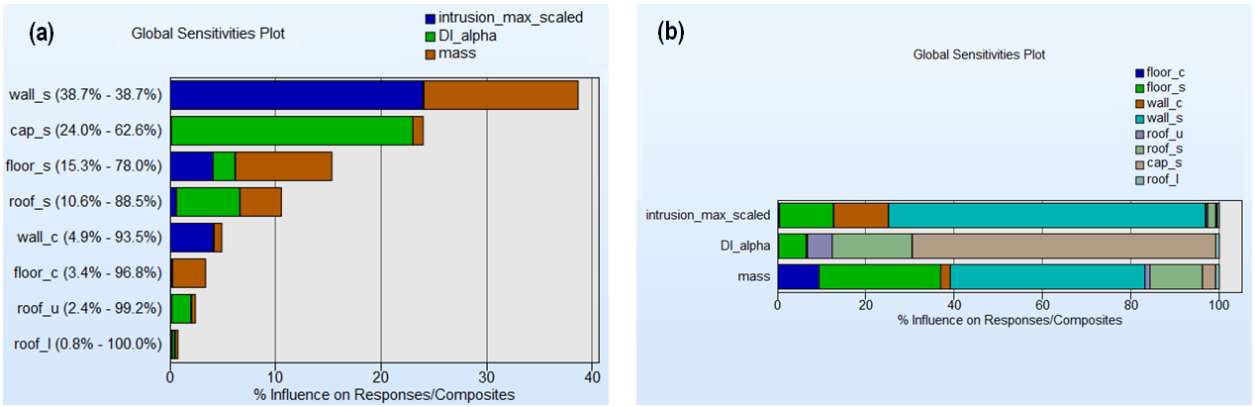

Figure 12: Cumulative global sensitivity study (a) direct view (b) transposed view

4.3. Trade-off Study

Figure 13 presents trade-off studies for *DI* versus *mass* and for *intrusion_max_scaled* versus *mass* objectives. All the points marked with triangles are generated based on the metamodels. Twenty-eight (points marked with squares were generated based on the direct LS-DYNA simulations. Also, the initial and "most optimal" designs are highlighted.

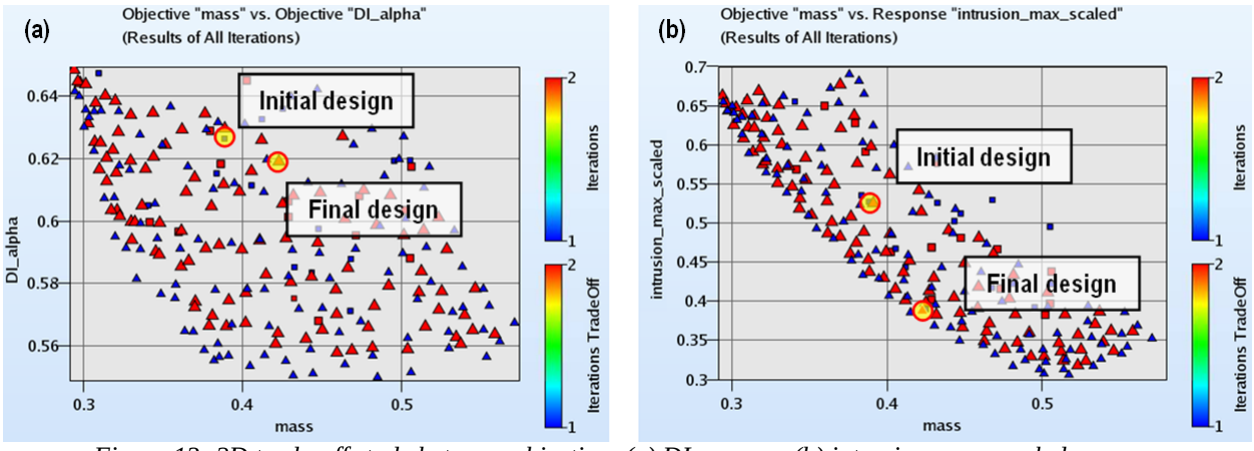

Figure 13: 2D trade-off study between objectives (a) DI vs. mass (b) intrusion_max_scaled vs. mass

In real life problems, designers need to consider additional preference information in order to distinguish between the Pareto solutions. Methods for visualization of the high dimensional data sets were recently a subject for study and the current state of the art can be found in [6]. LS-OPT 4.1 offers the following methods for visualization of *n*-dimensional data: 3D trade-off plots, Hyper-Radial Visualization (HRV), Parallel Coordinate Plot and Self Organizing Maps [4].

In this study, HRV maps the multi-objective optimization problem defined by Equations (2) and (3) into a single objective optimization problem defined by Equations (10) and (11):

$$\text{minimize:} \qquad \frac{\sum_{i=1}^{s} W_i \tilde{F}_i^2 + \sum_{i=s+1}^{n} W_i \tilde{F}_i^2}{s} \tag{10}$$

$$\text{subject to:} \qquad \sum_{i=1}^{n} W_i = 1 \text{ and } W_i > 0 \tag{11}$$

Where:

$$\tilde{F}_i = \frac{f_i(\boldsymbol{x}) - f_{i\min}(\boldsymbol{x})}{f_{i\max}(\boldsymbol{x}) - f_{i\min}(\boldsymbol{x})} \qquad i = 1,\ldots,n \qquad \text{and } \tilde{F}_i \in [0,1] \tag{12}$$

Using transformation (12), *s* functions are represented by Hyper-Radial Calculation 1 (HRCW1) and *n* – *s* functions are represented by HRCW2 given by:

$$HRCW1 = \sqrt{\frac{\sum_{i=1}^{s} W_i \tilde{F}_i^2}{s}} \qquad \text{and} \qquad HRCW2 \sqrt{\frac{\sum_{i=s+1}^{n} W_i \tilde{F}_i^2}{n-s}} \tag{13}$$

Where:

W_i – preference weights.

Figure 14 shows the HRV plot for the objective functions. These results were obtained with all preference weights equal to 1.0. The point closest to the origin (0, 0) denotes the best solution in the HRV sense. Values of the objectives for this design are compared to the initial values in

Table 4. The *mass* objective increased by 9 %, and the *DI* decreased by ~2 %. *Intrusion_max_scaled* decreased by ~26 %.

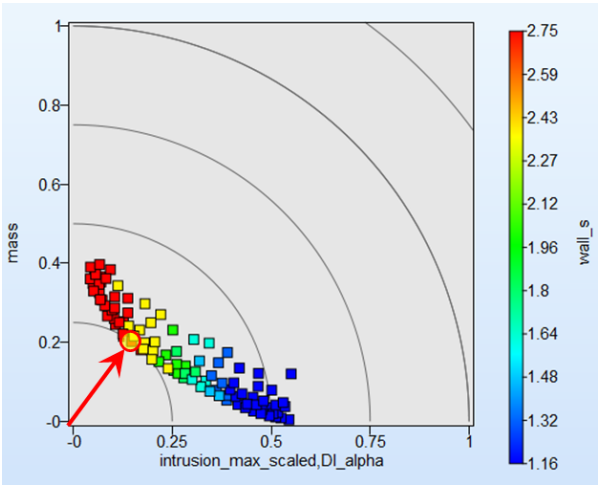

Figure 14: HRV plot for three objective functions

Table 4: Optimal design obtained from HR optimization

Objective	***Initial design***	***Optimal design***
mass	0.388 tonne	0.423 tonne
DI	0.63	0.62
intrusion_max_scaled	0.53	0.39

5. Conclusions

This paper presents results of a multi-objective optimization of the bus structure subject to rollover and side impact test simulations. Linear ANOVA and Sobol's Indices were used to identify and rank the most relevant elements of the structure for the objectives considered. The most important design variables were: thicknesses of the side wall tubes (*wall_s*) and front cap structure (*cap_s*). Variations in these input variables were responsible for ~63 % of the overall variations in the objective functions.

The initial design of the bus structure passed both rollover and side impact virtual tests. However, as shown in the study, increase of the bus frame mass by 9.0 % (0.7 % of total bus mass) and appropriate mass redistribution may decrease the maximum side impact intrusion by ~26%.

Acknowledgements

Argonne National Laboratory is a U.S. Department of Energy laboratory managed by UChicago Argonne, LLC. Argonne's Transportation Research and Analysis Computing Center (TRACC) is supported by the U.S. Department of Transportation. Argonne's TRACC wishes to acknowledge Dawn Tucker-Thomas of the U.S. DOT Research and Innovative Technology Administration for supporting this work. The authors acknowledge the strong support for this research from TRACC's Director, Dr. David P. Weber. The authors would also like to express their appreciation to Robert Westbrook from the Transit Office of the Florida DOT and Dr. Jerry Wekezer from FAMU-FSU College of Engineering for providing the finite element model of the bus.

References

[1] Kwasniewski L., et al., *Crash and safety assessment program for paratransit buses*, International Journal of Impact Engineering, Pages 235-242, Volume 36, Issue 2, February 2009.

[2] UN-ECE Regulation 66, Addendum 65, *Uniform technical prescriptions concerning the approval of large passenger vehicles with regard to the strength of their superstructure* Feb, 22, 2006.

[3] Bojanowski C., et al., *Florida Standard for Crashworthiness and Safety Evaluation of Paratransit Buses*, 21st International Technical Conference on the Enhanced Safety of Vehicles, US DOT NHTSA , Paper No. 09-0299-O, Stuttgart, Germany, June 15-18, 2009

[4] Stander N. et al., *LS-OPT® User's Manual - A Design Optimization and Probabilistic Analysis Tool for the Engineering Analyst*, LSTC, Livermore, 2010.

[5] Archer G.E.B., Saltelli A., Sobol M.I., *Sensitivity Measures, ANOVA-Like Techniques and the Use of Bootstrap*, Journal of Statistical Computation and Simulation, Pages 99 – 120, Volume 58, Issue 2, 1997.

[6] Chiu P.W., Bloebaum C.L., *Hyper-Radial Visualization (HRV) Method with Range-Based Preferences for Multi-Objective Decision Making*, Journal of Structural and Multidisciplinary Optimization, Pages 97-115, Volume 40, Numbers 1-6, January, 2010.

The submitted manuscript has been created by UChicago Argonne, LLC, Operator of Argonne National Laboratory ("Argonne"). Argonne, a U.S. Department of Energy Office of Science laboratory, is operated under Contract No. DE - AC02 - 06CH11357. The U.S. Government retains for itself, and others acting on its behalf, a paid - up nonexclusive, irrevocable worldwide license in said article to reproduce, prepare derivative works, distribute copies to the public, and perform publicly and display publicly, by or on behalf of the Government.